Review Article

IJES *Iranian Journal of Earth Sciences*
Vol. 13, No. 3, 2021, 209-222.
DOI: 10.30495/ijes.2021.682866

Comparison of the Third- order moving average and least square methods for estimating of shape and depth residual magnetic anomalies

Mohammad Fouladi, Mirsattar Meshinchi Asl*, Mahmoud Mehramuz, Nima Nezafati

Department of Earth Sciences, Science and Research Branch, Islamic Azad University, Tehran, Iran

Received 18 November 2019; accepted 23 February2020

Abstract

In the current study, we have developed a new method called the third- order moving average method to estimate the shape and depth of residual magnetic anomalies. This method, calculates a nonlinear relationship between depth and shape factor, at seven points with successive window length. It is based on the computing standard deviation at depths that are determined from all residual magnetic anomalies for each value of the shape factor. The method was applied to the synthetic model by geometrical shapes both as horizontal cylinder and combination of horizontal cylinder, sphere and thin sheet approaches, with and without noise. It was tested by real data in Geological Survey of Iran (GSI). In this study, least square methods were applied to interpret the magnetic field so that we can compare the results of this methods with the third- order moving average method. This method is applied to estimate the depth using second horizontal derivative anomalies obtained numerically from magnetic data with successive window lengths. This method utilizes the variance of the depths as a scale for calculation of the shape and depth. The results showed that the third- order moving average method is a powerful tool for estimating shape and depth of the synthetic models in the presence and absence of noise compared to least square method. Moreover, the results showed that this method is very accurate for real data while the least square method did not lead to feasible results.

Keywords: *Residual magnetic anomalies, Third- order moving average, Least square method, Standard deviation, Variance.*

1. Introduction

Estimation of depth and shape is a crucial factor in magnetic data interpretation and many methods have been developed for this purpose. We can mention a method called Euler decomposition, whose calculations are solved independently based on depth and shape. Furthermore, a good review is provided by Hinze (1990) for estimating the depth of a buried structure of magnetic data. Several geometrical methods have been proposed for the interpretation of magnetic data due to the simple 2D-shapes such as sphere, cylinders, dikes and geological structures (Gay 1963; Paul 1964; Gay 1965; Radhakrishna Murthy 1967; Stanley 1977; Atchuta Roa and Ram Babu 1980; Prakasa Rao et al.1986; Prakasa Rao and Subrahmanyam 1988). However, none of the above studies discussed the accuracy and validity of the models in sufficient detail when the data are inherently noisy. Different numerical methods have been presented for determining the depth from magnetic data, such as Werner deconvolution method (Werner 1953; Hartman et al. 1971; Jain 1976) and Euler method (Thompson 1982; Reid et al. 1990). Moreover, these methods utilized linear equations for determination the depth of magnetic anomalies. The methods are sensitive to errors both in anomaly amplitude resolution and in determination of vertical and horizontal gradients, which are highly sensitive to noise (Steenland 1968). As a result, a suitable method for finding model parameters was presented by McGrath and Hood (1970) based on the least-squares method.

---

*Corresponding author.
E-mail address (es): m.meshinchi@srbiau.ac.ir

Abdelrahman and Abo-Ezz (2001) developed an approach for determination of the depth using numerical derivative anomalies. However, most of these methods are dependent upon initial estimation of the model parameters, but Abdelrahman et al. (2007) showed that least-squares method which was applied to estimate the depth, utilized numerical second horizontal derivative anomalies obtained from magnetic data with successive window lengths. They used the variance of the depths as a scale for calculating the shape and depth.

In addition, Abdelrahman and Essa (2015) presented a new method to estimate the shape and depth of residual magnetic anomalies for most geological structures. They extended a curved window method for simultaneous determination of shape and depth. They used second horizontal derivative anomalies obtained from magnetic data with of successive window lengths. But this method has limitations for estimation of shape and depth of buried structures in some cases. Their method cannot be applied to observed data consisting of the combined effect of a residual component due to a purely local structure and a regional component represented by a third- or fourth-order polynomial.

To solve the above problems, Abdelrahman et al. (2016) introduced ‘‘second moving average method’’ for the estimation of shape and depth using residual magnetic anomalies. They showed the magnetic anomaly by separate model due to a vertical and horizontal magnetic anomalies of the sphere, the horizontal cylinder, the thin sheet, and the geological contact. Pengfei et al (2017) introduced the Tilt-depth method, widely used to determinate the source depth of a magnetic anomaly.

They deduce similar Tilt-depth methods for both magnetic and gravity data based on the contact and sphere models and obtain the same equation for a gravity anomaly as that for a magnetic anomaly. They propose a weighting method based on the estimated depths from both the contact model and the sphere model to estimate the depth for real data. Then, Essa et al. (2018) showed a new algorithm to estimate parameters that controlled the source dimensions from magnetic anomaly profile data in the light of PSO (particle swarm optimization). Essa and Elhussein (2019) are developed the particle swarm optimization for determination of the depth due to inference of second moving average residual magnetic anomalies. This approach was used to remove the impact of the regional background up to the third-order polynomial by applying filters of successive window lengths.

In the present study, a new method is proposed to estimate the shape and depth of residual magnetic anomalies which is known as third- order moving average. In this work, we intend to compare the ability of our method with least squares method using residual magnetic anomalies with successive window lengths. Also, in this study we used synthetic models in magnetic field of horizontal cylinder model and combination of magnetic field of the horizontal cylinder, sphere and thin sheet models for comparison of the third- order moving average and least squares methods for estimating of shape and depth of the buried structures by residual magnetic anomalies.

2. Methodology

Many of the geological structures can be modeled as simple geometrical shapes like, sphere, cylinder, dike and geological contact. These four geometrical shapes, are almost similar to geological structures that often applied in the interpretation of magnetic data for the exploration. In this article, these four geometrical shapes shown in the Fig. 1, were used for the synthetic modeling. In addition, we will prove the mathematical relations of third-order moving average method while reviewing the mathematical relations of the least squares method. The total intensity, vertical and horizontal magnetic anomaly of the sphere and the horizontal cylinder are defined according to equation 1 (Abdelrahman and Essa 2015).

$$T\left(x_i,z\right)=K\frac{Az^{2}+Bx_i+Cx_i^{2}}{\left(x_i^{2}+z^{2}\right)^{q}} \qquad (1)$$

Where:

Model	Field component	A	B	C
Sphere	Total field	$3\sin^2\theta-1$	$-3z\sin 2\theta$	$3\cos^2\theta-1$
Sphere	Vertical field	$2\sin\theta$	$-3z\cos\theta$	$-\sin\theta$
Sphere	Horizontal field	$-\cos\theta$	$-3z\sin\theta$	$2\cos\theta$
Cylinder	Horizontal cylinder	$\cos\theta$	$2z\sin\theta$	$-\cos\theta$
Thin sheet (FHD), geological contact (SHD) for a thin sheet, geological contact (FHD)	Total, Vertical, Horizontal	$\cos\theta/z$	$-\sin\theta$	0

In equation 1, z is the depth from earth's surface to center of anomaly, x_i is the position coordinate, K is the amplitude factor, θ is an inclination parameter and q is the shape factor, FHD and SHD denote the first and the second horizontal derivatives of the magnetic anomaly, respectively.

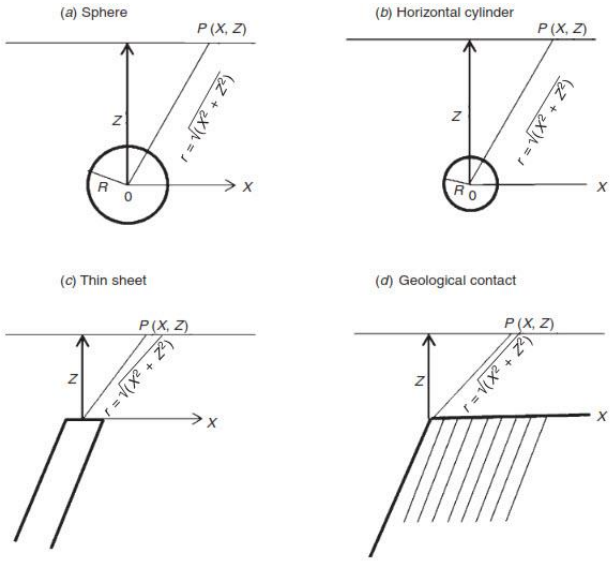

Fig 1. Geometrical shapes (Abdelrahman et al. 2016).

2.1. Third- order moving average method

This method, calculates a nonlinear relationship between depth and shape factor, at seven points with successive window lengths. It is based on the computing of standard deviation of depths that are determined from all residual magnetic anomalies for each value of the shape factor.

Using equation 1, the residual magnetic anomalies obtained from third- order moving average method are defined according to equation 2. In this equation, R_2 (Abdelrahman et al. 2016) and R_3 are the second- order and third- order moving average method along the anomaly profile, respectively and s is the window length that its unit is meter.

$$R_3(x_i,z,q,s)=R_2(x_i)-Z_3(x_i) \qquad (2)$$

Where:

$$R_2(x_i,z,q,s)=R_1(x_i)-z_2(x_i)$$

$$z_2(x_i)=\frac{R_1(x_i-s)+R_1(x_i+s)}{2},\quad for\rightarrow s=1,2,..,M$$

$$R_1(x_i,z,q,s)=T(x_i)-z_1(x_i)$$

$$z_1(x_i)=\frac{T(x_i-s)+T(x_i+s)}{2},\quad for\rightarrow s=1,2,..,N$$

$$R_2(x_i)=\frac{K}{2}\left\{\begin{array}{l}3\dfrac{Az^2+Bx_i+Cx_i^2}{(x_i^2+z^2)^q}-2\dfrac{Az^2+B(x_i-s)+C(x_i-s)^2}{((x_i-s)^2+z^2)^q}-2\dfrac{Az^2+B(x_i+s)+C(x_i+s)^2}{((x_i+s)^2+z^2)^q}\\+\dfrac{1}{2}\dfrac{Az^2+B(x_i-2s)+C(x_i-2s)^2}{((x_i-2s)^2+z^2)^q}+\dfrac{1}{2}\dfrac{Az^2+B(x_i+2s)+C(x_i+2s)^2}{((x_i+2s)^2+z^2)^q}\end{array}\right\}$$

$$\mathrm{Z}_3(\mathrm{x_i})=\frac{R_2(x_i-s)+R_2(x_i+s)}{2},\quad for\rightarrow s=1,2,..,\mathrm{N} \tag{3}$$

Where:

$$z_3(x_i)=\frac{K}{8}\left\{\begin{array}{c}7\dfrac{Az^2+B(x_i-s)+C(x_i-s)^2}{((x_i-s)^2+z^2)^q}-4\dfrac{Az^2+B(x_i-2s)+C(x_i-2s)^2}{((x_i-2s)^2+z^2)^q}\\-8\dfrac{Az^2+Bx_i+Cx_i^2}{(x_i^2+z^2)^q}+\dfrac{Az^2+B(x_i-3s)+C(x_i-3s)^2}{((x_i-3s)^2+z^2)^q}\\+7\dfrac{Az^2+B(x_i+s)+C(x_i+s)^2}{((x_i+s)^2+z^2)^q}-4\dfrac{Az^2+B(x_i+2s)+C(x_i+2s)^2}{((x_i+2s)^2+z^2)^q}\\+\dfrac{Az^2+B(x_i+3s)+C(x_i+3s)^2}{((x_i+3s)^2+z^2)^q}\end{array}\right\}$$

Now by replacing seven observation data, x_i-3s , x_i-2s , x_i-s , x_i , x_i+s , x_i+2s , x_i+3s in the equation 1, the residual magnetic anomalies are obtained by the third- order moving average method:

$$R_3(x_i,z,q,s)=\frac{K}{8}\left[\begin{array}{c}20\dfrac{Az^2+Bx_i+Cx_i^2}{(x_i^2+z^2)^q}-15\dfrac{Az^2+B(x_i-s)+C(x_i-s)^2}{((x_i-s)^2+z^2)^q}\\-15\dfrac{Az^2+B(x_i+s)+C(x_i+s)^2}{((x_i+s)^2+z^2)^q}\\+6\dfrac{Az^2+B(x_i-2s)+C(x_i-2s)^2}{((x_i-2s)^2+z^2)^q}\\+6\dfrac{Az^2+B(x_i+2s)+C(x_i+2s)^2}{((x_i+2s)^2+z^2)^q}\\-\dfrac{Az^2+B(x_i-3s)+C(x_i-3s)^2}{((x_i-3s)^2+z^2)^q}\\-\dfrac{Az^2+B(x_i+3s)+C(x_i+3s)^2}{((x_i+3s)^2+z^2)^q}\end{array}\right] \tag{4}$$

It is necessary to solve equation 4 for. $x_i=+2s$, $x_i=-2s$, $x_i=+3s$ and $x_i=-3s$ also by subtracting and division these equations, we are able to delete A, C and K,B respectively, So:

$$(4s^2+z^2)^q=\frac{40}{A+B} \tag{5}$$

Where:

$$E=\frac{R_3(+2s)-R_3(-2s)}{R_3(+3s)-R_3(-3s)}$$

$$A=\left\{\begin{array}{l}-\dfrac{30E}{(4s^2+z^2)^q}+\dfrac{6E}{(s^2+z^2)^q}+\dfrac{60E}{(9s^2+z^2)^q}\\-\dfrac{60E}{(16s^2+z^2)^q}+\dfrac{36E}{(25s^2+z^2)^q}-\dfrac{6E}{(36s^2+z^2)^q}\end{array}\right\}$$

$$B=\frac{14}{(s^2+z^2)^q}+\frac{45}{(9s^2+z^2)^q}-\frac{24}{(16s^2+z^2)^q}+\frac{5}{(25s^2+z^2)^q}$$

Finally, according to equation 5, we have:

$$z=\left\{\left(\frac{40}{A+B}\right)^{1/q}-4s^2\right\}^{1/2} \quad (6)$$

Equation 6 can be used for z using standard methods for nonlinear equations. In this study, in synthetic models, data were contaminated with random noise using equation 7 (Abdelrahman and Essa 2016). In this Equation, $T_{noise}(x_i)$ is the noisy magnetic field value at x_i, M is the noise amplitude factor, RAN is a random number between zero and one, profile length and sampling interval are 100 m and 1m, respectively.

$$T_{noise}(x_i)=T(x_i)+M\,(\mathrm{RAN(i)}-0.5) \quad (7)$$

According to the equation 6 and considering the different shape factors and the successive window length, the depth is calculated for each one. Then the average and standard deviation of the depths are calculated. From the obtained depths, the depth having the lowest standard deviation which is the depth of the anomaly and the shape factor in accordance with this depth, confirms the shape of the magnetic anomaly. Finally, we simultaneously determine the depth and shape of a buried structure obtained from magnetic data with filters of successive window lengths.

2.2. Least- Squares method

This method is based on the computing of variance of depths that are determined from all profiles which are second- derivative anomalies. Variance is a scale for determining the correct shape and depth of buried structure. The magnetic anomaly produced by most geological structures according to Gay (1963), Prakasa Rao et al. (1986) and Prakasa Rao and Subrahmanyan (1988) defined according to equation 8 (Abdelrahman et al. 2007).

$$T(X_i,Z,\theta)=K\frac{(aZ^{2r}+bX_i^{2})(\sin\theta)^m(\cos\theta)^n+cX_iZ^{p}(\sin\theta)^n(\cos\theta)^m}{(X_i^{2}+Z^{2})^q},\ i=1,2,3,\ldots N \quad (8)$$

In equation 8, z is the depth, X_i is the position coordinate (Centre located at $x_i=0$), K is the amplitude factor, θ is an inclination parameter and q is the shape factor. The numerical values for a,b,c,m,n,r,p,q for all of the models are given in Table 1. Since the total magnetic intensity of the sphere does not follow the equation 8, it was not presented in Table 1. Now by replacing five observation data, x_i-2s, x_i-s, x_i, x_i+s, x_i+2s along the anomaly profile. In the following, we must first calculate the second numerical horizontal derivative and then do that for all shapes at the origin $x_i=0$, obtained the equation 9: (Abdelrahman et al. 2007).

Table 1. The numerical values for geological structures

Model	Field component	*a*	*b*	*c*	*m*	*n*	*p*	*r*	*q*
Sphere	Vertical	2	-1	-3	1	0	1	1	2.5
Sphere	Horizontal	-1	2	-3	0	1	1	1	2.5
Horizontal cylinder, dike (FHD), geological contact (SHD)	Total, vertical, horizontal	1	-1	2	0	1	1	1	2
Dike, geological contact (FHD)	Total, vertical, horizontal	1	0	-1	0	1	0	0.5	1

$$T_{XX}(X_i,Z,\theta,S)=\frac{Z^{2q}T_{XX}(0)(4S^2+Z^2)^q}{2\left[Z^{2q}(aZ^{2r}+4bS^2)-aZ^{2r}(4S^2+Z^2)^q\right]}\times \left[\begin{array}{l}\dfrac{(aZ^{2r}+b(X_i+2S)^2)+c(X_i+2S)Z^{p})(\tan\theta)^{m-n}}{((X_i+2S)^2+Z^2)^q}\\ -2\dfrac{(aZ^{2r}+bX_i^{2})+cX_iZ^{p}(\tan\theta)^{m-n}}{(X_i^{2}+Z^{2})^q}\\ +\dfrac{(aZ^{2r}+b(X_i-2S)^2)+c(X_i-2S)Z^{p}(\tan\theta)^{m-n}}{((X_i-2S)^2+Z^2)^q}\end{array}\right] \quad (9)$$

Now, we will calculate the numerical derivative value for $x_i=\pm s$ and then according $F=\frac{T_{XX}(S)-T_{XX}(-S)}{T_{XX}(0)}$ we will have:

$$T_{XX}(X_i,Z,S)=\frac{T_{XX}(0)}{2}W(X_i,Z,S) \quad (10)$$

Where

$$W(X_i,Z,S)=Z^{2q}D(S,Z)[H(X_i,Z,S)-2U(X_i,Z,S)+\mathrm{V}(X_i,Z,S)]$$

$$H(X_i,\mathrm{Z},\mathrm{S})=\frac{(aZ^{2r}+b(X_i+2\mathrm{S})^2)+c(X_i+2S)Z^p)R(\mathrm{S},\mathrm{Z})}{((X_i+2S)^2+Z^2)^q}$$

$$U(X_i,S,Z)=\frac{(aZ^{2r}+bX_i^2)+cX_iZ^pR(S,Z)}{(X_i^2+Z^2)^q}$$

$$V(X_i,\mathrm{S},\mathrm{Z})=\frac{(aZ^{2r}+b(X_i-2\mathrm{S})^2)+c(X_i-2S)Z^pR(\mathrm{S},\mathrm{Z})}{((X_i-2S)^2+Z^2)^q}$$

$$D(S,Z)=\frac{(4S^2+Z^2)^q}{2\left[Z^{2q}(aZ^{2r}+4bS^2)-aZ^{2r}(4S^2+Z^2)^q\right]}$$

The unknown depth Z in equation 10 can be obtained by minimizing:

$$\psi(Z)=\sum_i^N\left[L(X_i)-\frac{T_{XX}(0)}{2}W(X_i,Z,S)\right]^2 \quad (11)$$

$\psi(Z)$ is minimizing the depth z, $L(X_i)$ is second horizontal derivative anomaly at X_i and $d(\psi(Z))/\mathrm{dZ}=0$ is Minimization of $\psi(Z)$ by least-squares.

$$f(Z)=\sum_i^N\left[L(X_i)-\frac{T_{XX}(0)}{2}W(X_i,Z,S)\right]W^*(X_i,Z,S)=0 \quad (12)$$

Where

$$W^*(X_i,Z,S)=d(W(X_i,Z,S))/dZ$$

Following, both the third order moving average method and least squares method were modeled synthetically by MATLAB software. These models were horizontal cylinder and combination of sphere, horizontal cylinder and thin sheet.

3. Synthetic Modeling

3.1. Magnetic field of horizontal cylinder model

The residual magnetic anomaly in Fig 2, demonstrate the magnetic field due to a horizontal cylinder ($K=4000nT, z=8m, \theta=30^\circ$ and $q=2$). In this model, the regional magnetic field is second- order polynomial (equation 13). For this reason, the regional magnetic field in Fig 2 is seen as a parabola curve (green curve).

The composite anomaly (residual magnetic anomaly of the horizontal cylinder and regional anomaly) for horizontal cylinder model (red curve) and residual magnetic anomaly (blue curve) are defined according to equation 14:

$$Regional\ magnetic\ field=0.02x^2+x+10 \quad (13)$$

$$T(x_i)=4000\frac{64\cos(30^\circ)+16x_i\sin(30^\circ)-x_i^2\cos(30^\circ)}{(x_i^2+64)^2}+0.02x^2+x+10 \quad (14)$$

Also, 5% random noise is added to residual magnetic field data (according to equation 7, M equals $5nT$). The black curve in Fig 2, shows a noisy magnetic field using four successive window lengths ($s=5,6,7$ and 8 spacing units). Fig 3 and 4, show values of the composite magnetic anomaly estimated using third- order moving average method without noise (red curve in Fig 2) and with noise (black curve in Fig 2) using four successive window lengths ($s=5,6,7$ and 8 spacing units), respectively. Also Fig 5 and 6, show the second numerical horizontal derivative values for non-noisy data and noisy data, respectively.

The values of the depth for composite magnetic anomaly by third- order moving average method and the second numerical horizontal derivative values by least- squares method, with and without noise were calculated by equations 6 and 11, respectively. Table 2 and Table 3, show the calculated depth values for the least- squares method and third- order moving average method by successive window lengths ($s=5,6,7$ and 8 spacing units) and different values of the shape factor, respectively. Table 2, shows that the minimum variance values by least- square method, obtained the $q=2$ for non- noisy data and the $q=1$ for noisy data. So, the shape of the magnetic anomaly by minimum variance value, is somehow between thin sheet structure and horizontal cylinder structure.

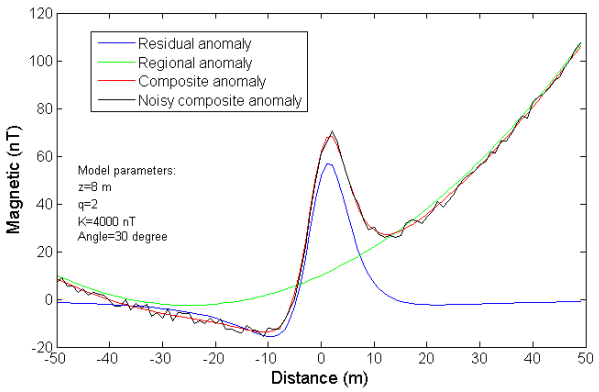

Fig 2. The magnetic field of a horizontal cylinder by $K=4000nT, z=8m$, $q=2$ and $\theta=30^\circ$ with regional magnetic field of two- order polynomial and random noise=5%

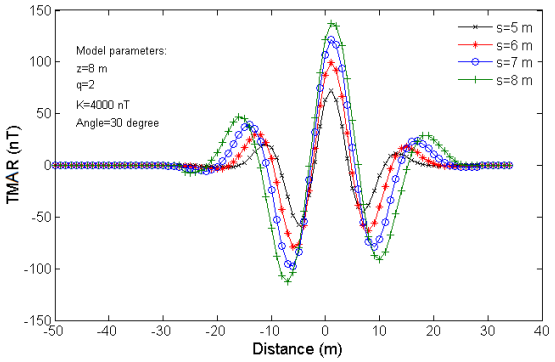

Fig 3. Values of the composite magnetic anomaly by third- order moving average method (TMAR) (without noise)

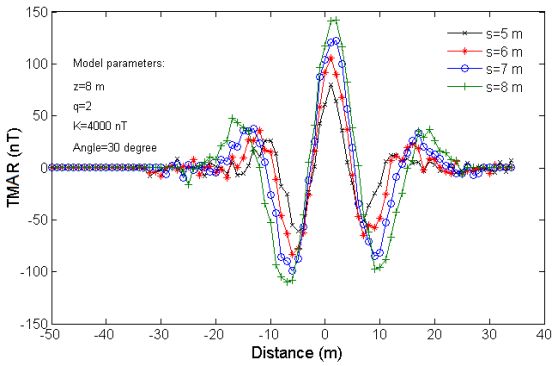

Fig 4. Values of the composite magnetic anomaly by third- order moving average method (TMAR) (with noise)

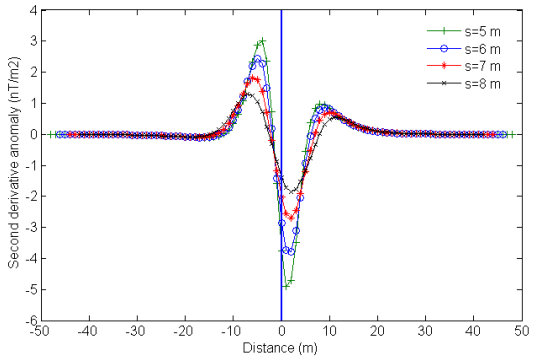

Fig 5. Values of the composite magnetic anomaly by least- squares method (Without noise)

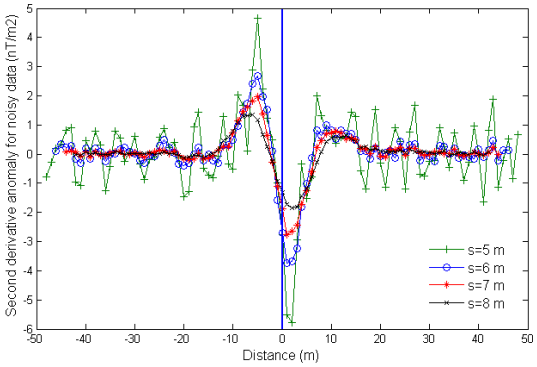

Fig 6. Values of the composite magnetic anomaly by least- squares method (With noise)

Table 2. The values of the depth for composite magnetic anomaly by least- squares method for successive window lengths ($s = 5, 6, 7$ and 8 spacing units) and different values of the shape factor. ($K = 4000nT, z = 8m, \theta = 30^{\circ}$ and random noise=5%). (The least variance shown in bold)

window length S (m)	Depth calculated for $q = 1$				Depth calculated for $q = 2$				Depth calculated for $q = 2.5$			
	Without noise	error %	With noise	error %	Without noise	error %	With noise	error %	Without noise	error %	With noise	error %
5	5.82	27.25	5.46	31.75	7.18	10.25	9.68	21	4.8	40	4.78	40.25
6	5.52	34.38	5.78	27.75	7.73	3.38	7.12	11	5.4	32.5	4.94	38.25
7	5.13	35.84	4.69	41.38	7.93	0.875	8.68	8.5	5.3	33.75	5.85	26.9
8	4.8	40	5.17	35.38	8	0	8.86	10.75	5.8	27.5	6.34	20.75
Average value (m)	5.32	33.53	5.28	34.06	7.71	3.63	8.59	7.38	5.17	35.38	5.48	31.5
variance (m^2)	0.199		**0.214**		**0.138**		1.14		0.169		0.553	

According to the Table 3, the minimum standard deviation for the estimated depths was obtained based on the shape factor for the non-noisy and noisy magnetic data equals 2 and 1.9, respectively. Hence, using the third-order moving average method, the closest depth to a given depth (average value) for non-noisy and noisy magnetic data was 8 m and 8.15 m, respectively. So, the shape of the magnetic anomaly by minimum standard deviation value, is the horizontal cylinder structure. Comparing Table 2 and Table 3 to estimate the shape and depth of buried structures, it can be concluded that third-order moving average method has a good agreement than the least squares method for the horizontal cylinder structure.

Table 3. The calculated depth values for successive window lengths (s=5,6,7 and 8 spacing units) and different values of the shape factor. ($K=4000nT, z=8m, \theta=30^{\circ}$ and random noise=5%). (The closest depth to a given depth shown in bold)

shape factor		S = 5	S = 6	S = 7	S = 8	Average value (m)	Standard deviation (m)
1.6	Without noise	6.43	6.88	6.63	6.58	6.63	0.187
	with noise	5.76	6.59	4.38	6.96	5.92	1.144
1.7	Without noise	6.58	7.24	6.83	7.77	7.12	0.52
	with noise	7.26	8.75	5.87	5.38	6.8	1.52
1.8	Without noise	7.71	7.37	7.06	7.69	7.46	0.31
	with noise	6.35	9.45	7.62	8.68	8.02	1.345
1.9	Without noise	7.86	7.67	7.34	7.85	7.68	0.243
	with noise	8.25	9.07	7.45	7.82	8.15	**0.7**
2	Without noise	8	8	8	8	8	**0**
	with noise	8.77	8.96	7.32	9.43	8.62	0.91
2.1	Without noise	8.05	8.23	7.78	8.1	8.04	0.19
	with noise	8.96	9.14	8.37	10.21	9.17	0.767
2.2	Without noise	8.17	8.38	7.95	8.24	8.19	0.18
	with noise	7.58	10.75	8.12	9.69	9.04	1.452
2.3	Without noise	8.22	8.54	8.13	8.41	8.33	0.185
	with noise	8.78	9.79	9.57	11.45	9.9	1.12
2.4	Without noise	8.43	8.69	8.26	8.57	8.49	0.185
	with noise	9.46	10.36	8.87	12.23	10.23	1.47

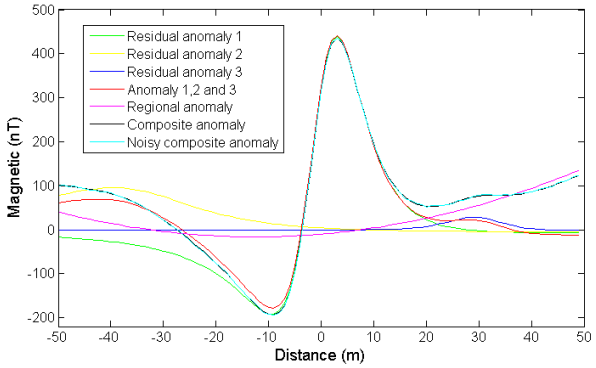

Fig 7. The magnetic field due to a horizontal cylinder by $K=50000nT, z=10m$ and $\theta=50^{\circ}$ (residual anomaly 1), vertical magnetic field of sphere by $K=25000nT, z=12m$ and $\theta=75^{\circ}$ (residual anomaly 2) and magnetic field of a thin sheet $K=2000nT, z=20m$ and $\theta=25^{\circ}$ (residual anomaly 3), with regional magnetic field of two- order polynomial and random noise=5%

3.2. Magnetic field of the horizontal cylinder, sphere and thin sheet models

Fig 7, shows the residual magnetic anomaly, magnetic field due to a horizontal cylinder by $K=50000nT, z=10m$ and $\theta=50^{\circ}$ (residual anomaly 1), vertical magnetic field of sphere by $K=25000nT, z=12m$ and $\theta=75^{\circ}$ (residual anomaly 2) and magnetic field of a thin sheet $K=2000nT, z=20m$ and $\theta=25^{\circ}$ (residual anomaly 3). The center of the horizontal cylinder model is at the origin of the profile and the center of the spherical model is 30 m from the origin and to the right and center of the thin sheet model is 35 m from the origin and to the left.

In these models, the regional magnetic field are considered two-order polynomial (Equation 15), a random noise of 5% and a successive window length $s=3,4$ and 5 spacing units.

In Fig 7, shows the regional magnetic field by purple curve, residual magnetic anomaly due to a horizontal cylinder by green curve, sphere model by yellow curve, thin sheet model by blue curve, composite anomaly without noise by black curve and composite anomaly with noise by turquoise curve.

The composite anomaly (residual magnetic anomaly of the horizontal cylinder, residual magnetic anomaly of the Sphere, residual magnetic anomaly of the thin sheet and regional anomaly) are defined according to equation 16:

$$Regional\ magnetic\ field = 0.04x^2 + x - 10 \qquad (15)$$

$$T(x_i) = 50000\frac{100\cos(50^{\circ}) - 20x_i\sin(50^{\circ}) - x_i^2\cos(50^{\circ})}{(x_i^2+100)^2} + 25000\frac{288\sin(75^{\circ}) - 36x_i\cos(75^{\circ}) - x_i^2\sin(75^{\circ})}{(x_i^2+144)^{2.5}} + 2000\frac{20\cos(25^{\circ}) - x_i^2\sin(25^{\circ})}{(x_i^2+400)} + 0.04x_i^2 + x_i - 10 \qquad (16)$$

Fig 8, 9, 10 and 11 show values of the composite magnetic anomaly by third- order moving average method without and with noise and the second numerical horizontal derivative values for non- noisy data and noisy data using three successive window lengths ($s=3,4$ and 5 spacing units), respectively. Also, Table 4 and 5, show the calculated values of the depth for the least- squares method and third- order moving average method with and without noise by successive window lengths ($s=3,4$ and 5 spacing units) and different values of the shape factor, respectively.

Table 4, shows that the minimum variance values by least- square method, obtained the $q=2$ for noisy data and the $q=1$ for non- noisy data. So, the shape of the magnetic anomaly by minimum variance value, is somehow between thin sheet structure and horizontal cylinder structure.

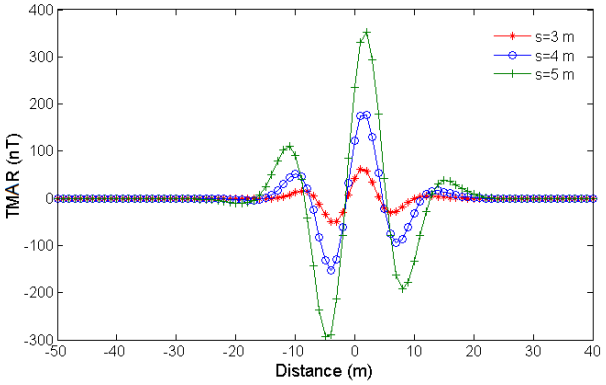

Fig 8. Values of the composite magnetic anomaly by third- order moving average method (TMAR) (without noise).

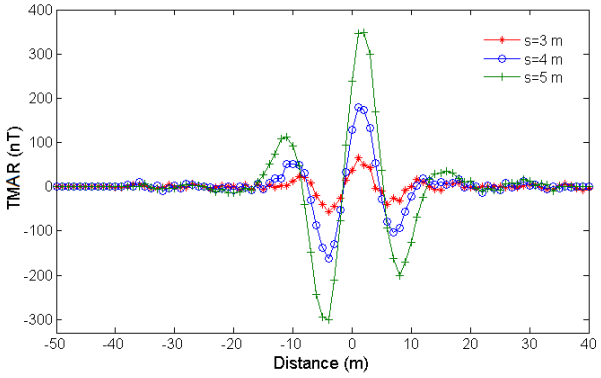

Fig 9. Values of the composite magnetic anomaly by third- order moving average method (TMAR) (with noise).

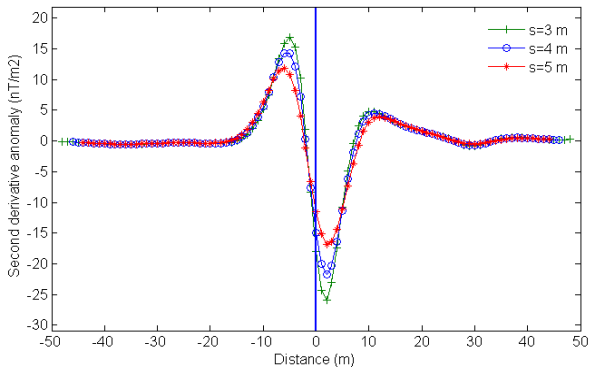

Fig 10. Values of the composite magnetic anomaly by least- squares method (Without noise).

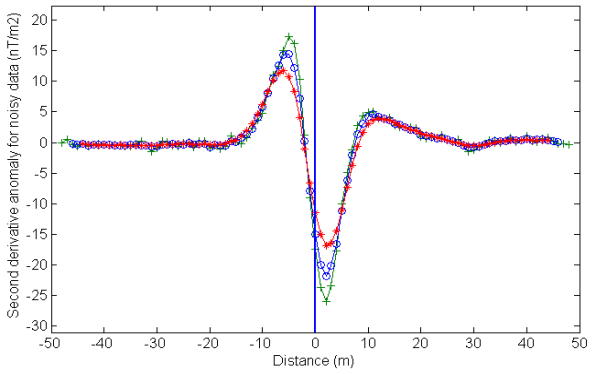

Fig 11. Values of the composite magnetic anomaly by least- squares method (With noise).

Table 4. The values of the depth for composite magnetic anomaly by least- squares method for successive window lengths (s=3,4 and 5 spacing units) and different values of the shape factor. ($K=50000nT, z=10m$ and $\theta=50^{\circ}$ (residual anomaly 1), $K=25000nT, z=12m$ and $\theta=75^{\circ}$ (residual anomaly 2), $K=2000nT, z=20m$ and $\theta=25^{\circ}$ (residual anomaly 3), random noise=5%,)). (The least variance shown in bold)

window length **S (m)**	Depth calculated for $q=1$				Depth calculated for $q=2$				Depth calculated for $q=2.5$			
	Without noise	error %	With noise	error %	Without noise	error %	With noise	error %	Without noise	error %	With noise	error %
3	7.29	27.1	7.47	25.3	9.44	5.6	9.36	6.4	6.63	33.7	6.04	39.6
4	7.05	29.5	7.27	27.3	10.33	3.3	9.64	3.6	7.01	29.9	7.37	26.3
5	6.68	33.2	6.02	39.8	10.74	7.4	10.59	5.9	7.07	29.3	6.41	35.9
Average value (m)	7	29.93	6.92	30.8	10.17	1.7	9.86	1.37	6.9	30.97	6.61	33.93
variance (m^2)	**0.0944**		0.786		0.665		**0.645**		0.239		0.686	

According to the Table 5, the minimum standard deviation for the estimated depths was obtained based on the shape factor for the non-noisy and noisy magnetic data equals 2 and 2.1, respectively. As a result, the shape of the magnetic anomaly by minimum standard value is the horizontal cylinder structure. So, when we compare Table 4 and 5 to estimate the shape and depth of the buried structures, it can be seen that the third-order moving average method has a good agreement for the horizontal cylindrical structure.

Table 5. The calculated values of the depth for composite magnetic anomaly by third- order moving average method for successive window lengths (S=3,4 and 5 spacing units) and different values of the shape factor. ($K = 50000nT, z = 10m$ and $\theta = 50^{\circ}$ (residual anomaly 1), $K = 25000nT, z = 12m$ and $\theta = 75^{\circ}$ (residual anomaly 2), $K = 2000nT, z = 20m$ and $\theta = 25^{\circ}$ (residual anomaly 3), random noise=5%,)). (The closest depth to a given depth shown in bold)

shape factor		S = 3	S = 4	S = 5	Average value (m)	Standard deviation (m)
1.6	Without noise	9.26	8.93	8.85	9.01	0.217
	with noise	8.38	7.82	7.47	7.89	0.46
1.7	Without noise	9.41	9.24	9.1	9.25	0.155
	with noise	8.74	8.47	7.96	8.39	0.396
1.8	Without noise	9.57	9.43	9.37	9.46	0.103
	with noise	9.29	8.84	9.05	9.06	0.226
1.9	Without noise	9.73	9.65	9.6	9.66	0.066
	with noise	9.61	9.16	9.44	9.4	0.23
2	Without noise	9.81	9.77	9.74	9.77	**0.0351**
	with noise	9.88	9.47	9.67	9.673	0.205
2.1	Without noise	9.96	10.08	9.85	9.963	0.115
	with noise	9.84	9.73	10.1	9.89	**0.19**
2.2	Without noise	10.17	10.35	10.27	10.26	0.09
	with noise	10.13	10.56	10.42	10.37	0.219
2.3	Without noise	10.32	10.67	10.48	10.49	0.175
	with noise	10.36	10.83	10.66	10.62	0.238
2.4	Without noise	10.55	10.87	10.63	10.683	0.166
	with noise	10.75	11.14	10.83	10.91	0.206

4. Real data

4.1. Geological Survey of Iran (Geophysics Site)

In order to study geomagnetic studies, an anomaly have been buried in the geophysical site of the Geological Survey of Iran that the information's of this anomaly are shown in Table 6. It should be noted that, the inside and outside of the buried anomaly is metal. Fig 12, show a picture of anomaly on the geophysics site of the geological survey of Iran. The magnetic measurements of the study area were shown in Tehran geological map on the scale of 1:100000 .Most of geological units in the study area are, alluvial sediments and Fans (Fig. 13). Also, Fig 14 shows the location of the study area (red square) and access routes.

Table 6. The information's of the magnetic anomaly

shape of the magnetic anomaly	Lengths of the magnetic anomaly	diameter of the magnetic anomaly	depth from Earth's surface to the lower surface of anomaly (m)	depth from Earth's surface to center of the anomaly (m)
Horizontal Cylinder	1.8	0.56	2.06	1.78

4.2. Geophysical data acquisition and data processing

The magnetic surveying, with one device (GSM-19T Proton Precession magnetometer) were measured in the field. In this site, spacing between profiles (East- West) and stations were selected as 0.5 m. Survey extent in geophysics site is 8 m*8.5 m that profiles number and stations number were measured 17 and 323, respectively. Fig 15, shows the total magnetic intensity map and the maximum and minimum values of the total magnetic intensity equals $47048nT$ and $43645nT$, respectively. For the correction of the magnetic data in this site, the magnetic residual map, local magnetic residual map (by remove a trend surface first- order) and reduced to magnetic pole map was prepared that Fig 16, show the reduced to magnetic pole map (according to the IGRF, regional magnetic field= $48451nT$, inclination= 54.66° and declination= 4.82°).

4.3. Application of the third- order moving average method

To analyze the magnetic field by the third- order moving average method, we introduce profile AA´ with length equal to 6.625 m on the local residual magnetic map (Fig17). According to the equation (15), the third- order moving average method with different window lengths was determined and plotted. Fig 18 and Table. 7 show the magnetic anomaly diagram and the calculated depth values for successive window lengths ($s = 0.1, 0.125, 0.15, 0.175$ and 0.2 spacing units) for profile AA´ using the third- order moving average method, respectively.

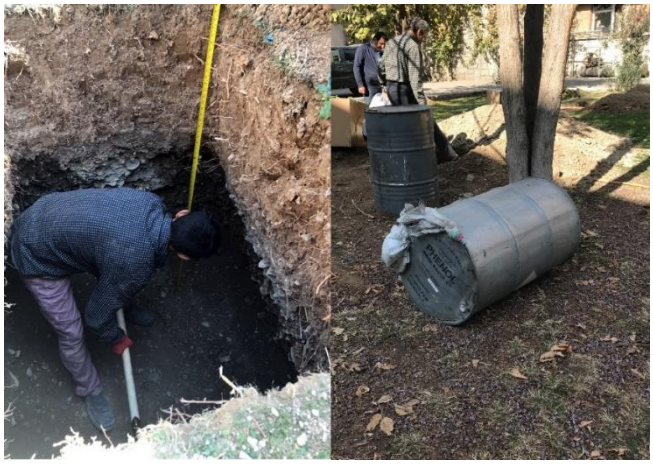

Fig 12. A picture of the magnetic anomaly on the geological survey of Iran.

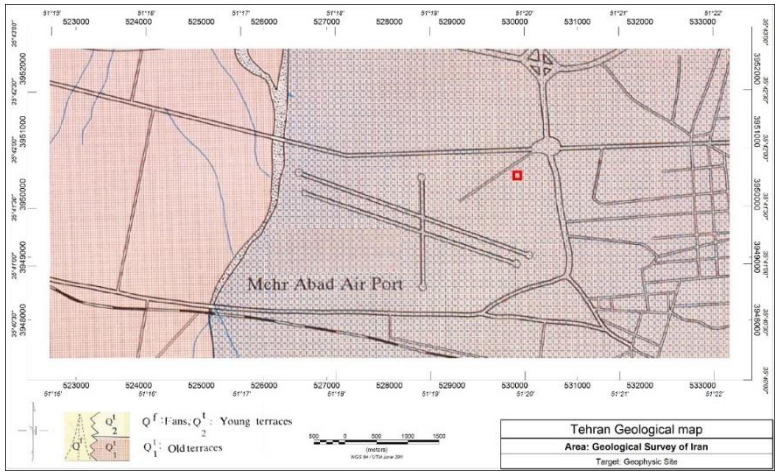

Fig 13. Geological map of magnetic anomaly area (red square), Geological Survey of Iran (1993).

Fig 14. Location of the study area (red square) and access routes (Google Earth)

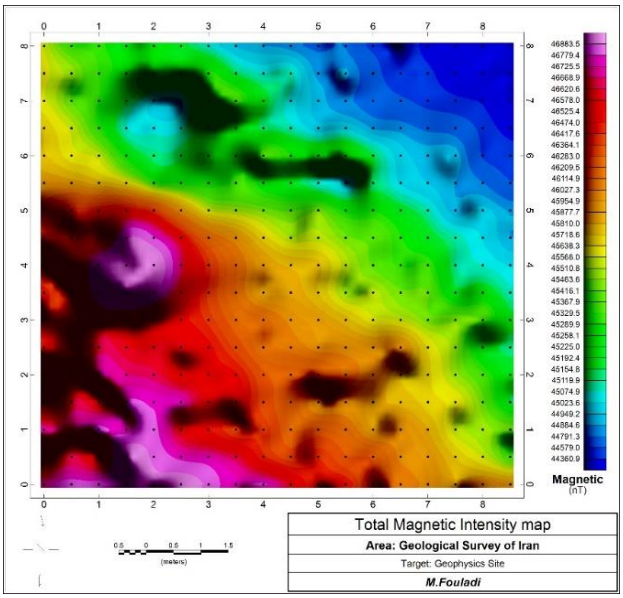

Fig 15. The total magnetic intensity map

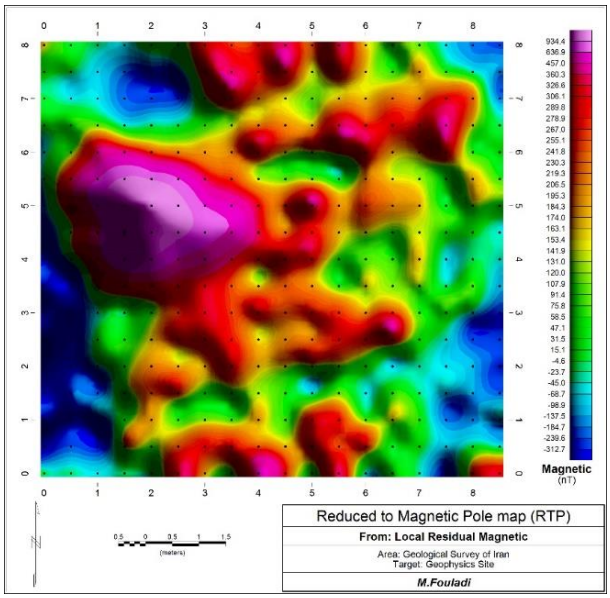

Fig 16. The reduced to magnetic pole map (RTP)

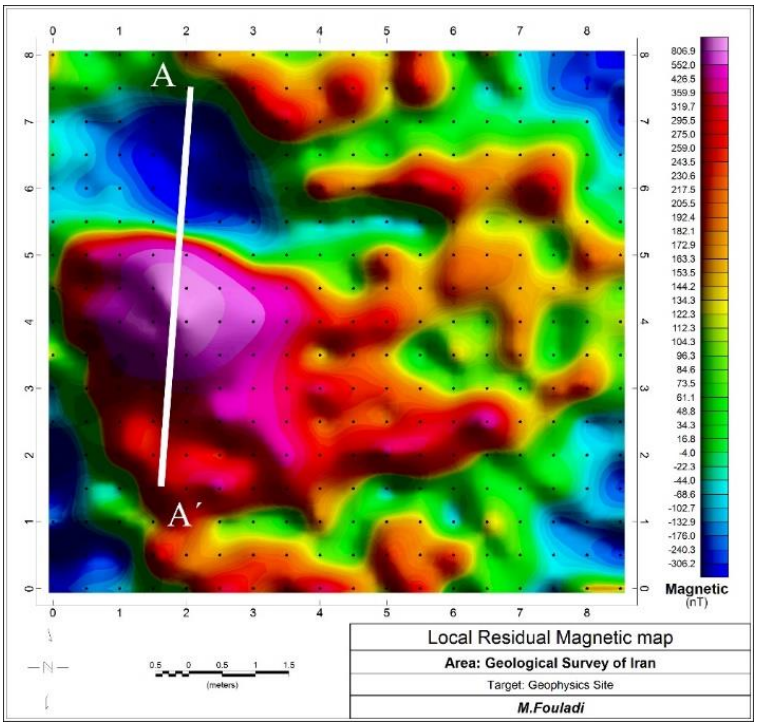

Fig 17. The profile AA´ on the local residual magnetic map

According to the Table 7, the minimum standard deviation for the estimated depths with different window lengths was obtained based on the shape factor equal to 2 the factor which is a horizontal cylinder structure. So based on the third- order moving average method, the mean depth of the anomaly for magnetic data obtained was 1.676 m.

4.4. Application of the least- square method

Using by equation 23, were determined and plotted numerical second horizontal derivative anomalies for successive window lengths ($s = 0.1, 0.125, 0.15, 0.175$ and 0.2 spacing units) for profile AA´ by utilizing the least- square method. Fig 19, shows the numerical second horizontal derivative magnetic anomalies. Results of the inversion with the least squares method for shape factor

1, 2 and 2.5 were show in table 8. This method is based on computing the variance of depths that are determined from all residual magnetic anomalies for each value of the shape factor with successive window length.
According to the Table 8, the minimum variance for the estimated depths with successive window lengths $s = 0.1, 0.125, 0.15, 0.175$ was obtained based on the shape factor for equal to 1, that show the shape of the anomaly is dike. Also, the estimated depth for this model, is 0.11m. While, according to prior information, the shape and depth of the anomaly in the geophysics site, is horizontal cylinder and 1.2m, respectively.

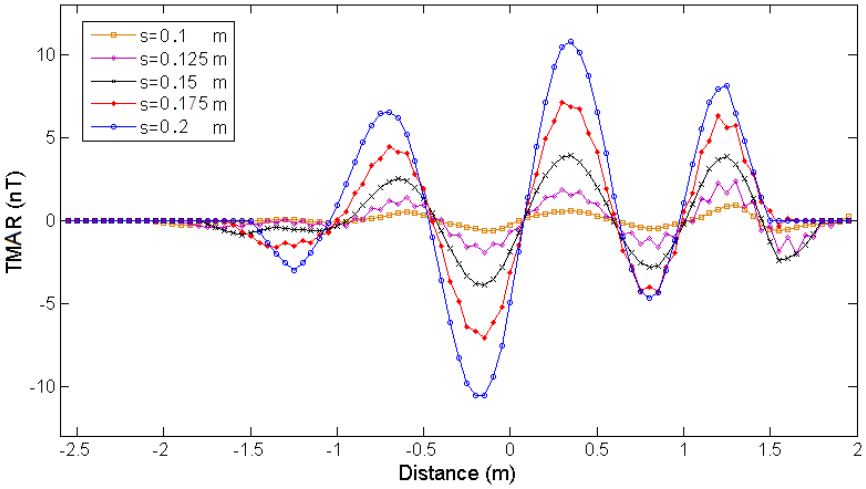

Fig 18. The magnetic anomaly by third- order moving average method (TMAR) (profile AA´)

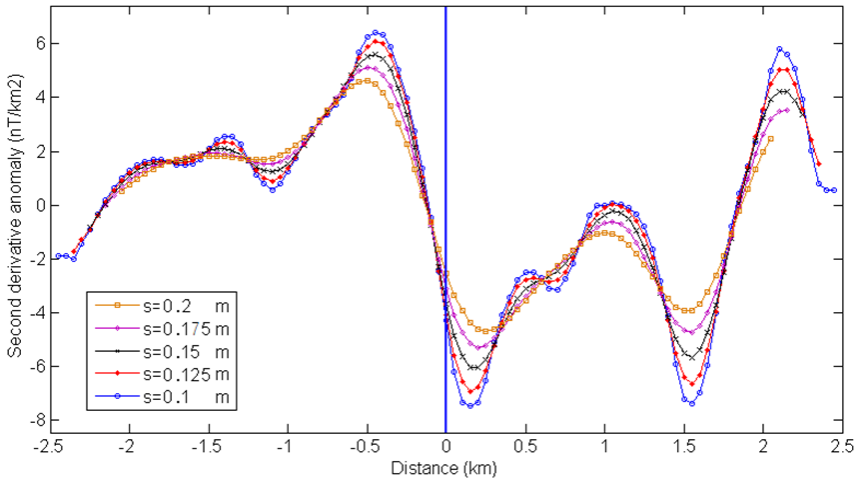

Fig 19. The numerical second horizontal derivative magnetic anomalies (profile AA´)

Table 7. The calculated shape factor and depth values for successive window lengths ($s = 0.1, 0.125, 0.15, 0.175$ and 0.2 spacing units) for profile AA´ by utilizing the third- order moving average method. (The closest depth to the actual depth is shown in bold)

shape factor	S = 0.1	S = 0.125	S = 0.15	S = 0.175	S = 0.2	Average value (m)	Standard deviation (m)
1.7	1.82	1.54	1.49	1.45	1.6	1.58	0.1454
1.8	1.84	1.56	1.51	1.49	1.64	1.608	0.1420
1.9	1.86	1.59	1.53	1.51	1.67	1.632	0.1418
2	**1.9**	**1.63**	**1.577**	**1.557**	**1.72**	**1.676**	**0.1398**
2.1	1.91	1.64	1.58	1.56	1.73	1.684	0.1426
2.2	1.93	1.65	1.6	1.58	1.77	1.706	0.1454
2.3	1.95	1.68	1.63	1.6	1.8	1.732	0.1438
2.4	1.97	1.7	1.64	1.63	1.81	1.75	0.1423

Table 8. The values of the depth for magnetic anomaly by least- squares method for profile AA´ with successive window lengths ($s = 0.1, 0.125, 0.15, 0.175$ and 0.2 spacing units) and different values of the shape factor. (The least variance shown in bold)

window length S (m)	Depth calculated for $q = 1$	Depth calculated for $q = 2$	Depth calculated for $q = 2.5$	Depth calculated for $q = 2.5$
	Dike model (all fields)	Horizontal cylinder (all fields)	Sphere (vertical field)	Sphere (horizontal field)
0.1	0.12	1.83	0.32	1.83
0.125	0.11	0.4	0.31	1.56
0.15	0.1	0.53	1.8	1.61
0.175	0.11	1.45	2	1.71
0.2	0.11	1.8	2.4	1.91
Average value (m)	0.11	1.2	1.11	1.724
variance (m^2)	**0.00004**	0.382	0.774	0.0172

5. Conclusions

The results showed that third- order moving average method, gives more accurate response in the absence of noise by the horizontal cylinder model for synthetic data and also shows a 2.3% error margin in the combined shape (horizontal cylinder, sphere (vertical field) and thin sheet models). Also, in the presence of noise for horizontal cylinder model and combination of horizontal cylinder, sphere (vertical field) and thin sheet models, errors were calculated 1.87% and 1.1%, respectively. But result of the least squares methods, can be shown that in the absence of noise by the horizontal cylinder model and combined shape for synthetic data, were errors calculated 3.63% and 29.93%, respectively. Also, this value with noise data, were obtained 34.06% and 1.37% error, respectively. The third- order moving average and least square methods has shown that for real magnetic data with 5% and 90.8% error, respectively (According to table 6).

Comparing the third- order moving average and least square methods defined that the third- order moving average is a powerful tool for estimating of shape and depth of the synthetic models and real data in the presence and absence of noise.

Acknowledgement

We sincerely thank the Geological Survey of Iran (GSI) for providing data and the possibility of Geophysical data acquisition on the Geophysics site.

References

Abdelrahman EM, Abo-Ezz ER (2001) Higher derivatives analysis of 2-D magnetic data, *Geophysics* 66: 205–212.

Abdelrahman EM, Abo-Ezz ER, Essa KS, El-Araby TM, Soliman KS (2007) A new least-squares minimization approach to depth and shape determination from magnetic data, *Geophysical Prospecting* 55: 433–446.

Abdelrahman EM, Essa KS (2015) A new method for depth and shape determinations from magnetic data, *Pure and Applied Geophysics* 172: 439–460.

Abdelrahman EM, Essa KS, El-Araby TM, Abo-Ezz ER (2016) Depth and shape solutions from second moving average residual magnetic anomalies, *Exploration Geophysics* 43: 178–189.

Atchuta Rao DA, Ram Babu HV (1980) Properties of the relation figures between the total, vertical, and horizontal field magnetic anomalies over a long horizontal cylinder ore body, *Current Science* 49: 584–585.

Essa KS, Elhussein M (2018) PSO (Particle Swarm Optimization) for Interpretation of Magnetic Anomalies Caused by Simple Geometrical Structures, *Pure and Applied Geophysics* 175(2).

Essa KS, Elhussein M (2019) Interpretation of Magnetic Data Through Particle Swarm Optimization: Mineral Exploration Cases Studies, *Natural Resources Research* 29: 521-537.

Gay P (1963) Standard curves for interpretation of magnetic anomalies over long tabular bodies, *Geophysics*, 28: 161–200.

Gay P (1965) Standard curves for interpretation of magnetic anomalies over long horizontal cylinders, *Geophysics* 30: 818–828.

Hartman RR, Teskey DJ, Friedberg JL (1971) A system for rapid digital aeromagnetic interpretation, *Geophysics* 36: 891–918.

Hinze WJ (1990) The role of gravity and magnetic methods in engineering and environmental studies, *Geotechnical and Environmental Geophysics* 75–126.

Jain S (1976) An automatic method of direct interpretation of magnetic profiles, *Geophysics* 41: 531–541.

McGrath PH, Hood PJ (1970) The dipping dike case: A computer curve-matching method of magnetic interpretation, *Geophysics* 35:831–848.

Paul PA (1964) Depth rules for some geometric bodies for interpretation of aeromagnetic anomalies, *Geophysics Research Bulletin* 2:15–21.

Pengfei L, Tianyou L, Peimin Z, Yushan Y, Qiaoli Z, Henglei Z, Guoxiong C (2017) Depth Estimation for Magnetic/Gravity Anomaly Using Model Correction, *Pure and Applied Geophysics* 174: 1729–1742.

Prakasa Rao TKS, Subrahmanyan M, Srikrishna Murthy A (1986) Nomograms for the direct

interpretation of magnetic anomalies due to long horizontal cylinders, *Geophysics* 51: 2156–2159.

Prakasa Rao TKS, Subrahmanyan M (1988) Characteristic curves for inversion of magnetic anomalies of spherical ore bodies, *Pure and Applied Geophysics* 126: 69–83.

Radhakrishna Murthy IV (1967) Note on the interpretation of magnetic anomalies of spheres, *I. G. U.* 4: 41–42.

Reid AB, Allsop JM, Granser H, Millett AJ, Somerton IW (1990) Magnetic interpretation in three dimensional using Euler deconvolution, *Geophysics* 55: 80–91.

Stanley JM (1977) Simplified magnetic interpretation of the geologic contact and thin dike, *Geophysics* 42: 1236–1240.

Steenland NC, Slack HA, Lynch VM, Langan L (1968) Discussion on The geomagnetic gradiometer, *Geophysics* 32: 877– 892.

Thompson DT (1982) EULDPH a new technique for making computer-assisted depth estimates from magnetic data, *Geophysics* 47: 31–37.

Werner S (1953) Interpretation of Magnetic Anomalies of Sheet-like Bodies, *Sveriges Geologiska Underok* Series C 43: N6.